MethodsX 14 (2025) 103175

Contents lists available at ScienceDirect

MethodsX

journal homepage: www.elsevier.com/locate/methodsx

Quantitative assessment of brain metabolism in mice using non-contrast MRI at 11.7T ☆,☆☆

Xiuli Yang, Yuguo Li, Hanzhang Lu, Zhiliang Wei*

Department of Radiology and Radiological Science, The Johns Hopkins University School of Medicine, United States

ARTICLE INFO

Method name:
Assessment of brain metabolism using non-contrast TRUST and PC MRI

Keywords:
Cerebral metabolic rate of oxygen (CMRO2)
Cerebral blood flow (CBF)
Fick principle
T2-relaxation-under-spin-tagging (TRUST)
Phase contrast (PC)

ABSTRACT

Brain oxygen metabolism indicates the rate of energy consumption and is a potential marker of pathological changes. Positron emission tomography (PET) is the gold standard for measuring metabolic rates using radioactive tracers. However, its application in preclinical studies, particularly with rodent animals, is constrained by the need for arterial input function measurements and on-site cyclotron facilities for tracer preparation. As an alternative, non-invasive, non-contrast MRI techniques, such as T2-relaxation-under-spin-tagging (TRUST) and phase-contrast (PC) MRI, can be used for evaluating brain metabolism in vivo. This study outlines a step-by-step method for implementing TRUST and PC MRI in mice at 11.7T scanner. The proposed method yields non-invasive, non-contrast quantitative measurements of global brain metabolism in approximately 20 min, paving the way for broader applications in future pathophysiological studies.

- Non-invasive and non-contrast assessment of brain metabolism in mice.
- Quantitative measurement of metabolic rate in approximately 20 min.

Specifications table

Subject area:	Neuroscience
More specific subject area:	Brain physiology
Name of your method:	Assessment of brain metabolism using non-contrast TRUST and PC MRI
Name and reference of original method:	N/A
Resource availability:	MATLAB codes are shared with the link below: https://github.com/zyliamwei/MouseCMRO2.

Background

The brain represents 2% of the total body weight but consumes approximately 20% of the body's energy, which is primarily supplied by aerobic metabolism [1]. Alterations in brain metabolism indicate critical pathophysiological changes, making it a promising biomarker for studying various pathologies, such as cardiac arrest [2] and Alzheimer's disease [3]. Positron emission tomography (PET) is the gold standard for evaluating brain metabolism in vivo. However, its reliance on invasive procedures to determine arterial input function and the need for an on-site cyclotron to prepare radioactive tracers limit its application, particularly in animal models.

☆ **Related research article:** None.

☆☆ **For a published article:** Wei Z, Roh SE, Yang X et al. The impact of isoflurane anesthesia on brain metabolism in mice: An MRI and electroencephalography (EEG) study. NMR Biomed 2024; 37: e5260. DOI: 10.1002/nbm.5260.

* Corresponding author.
E-mail address: zhiliang.wei@jhu.edu (Z. Wei).

https://doi.org/10.1016/j.mex.2025.103175
Received 7 January 2025; Accepted 15 January 2025
Available online 16 January 2025

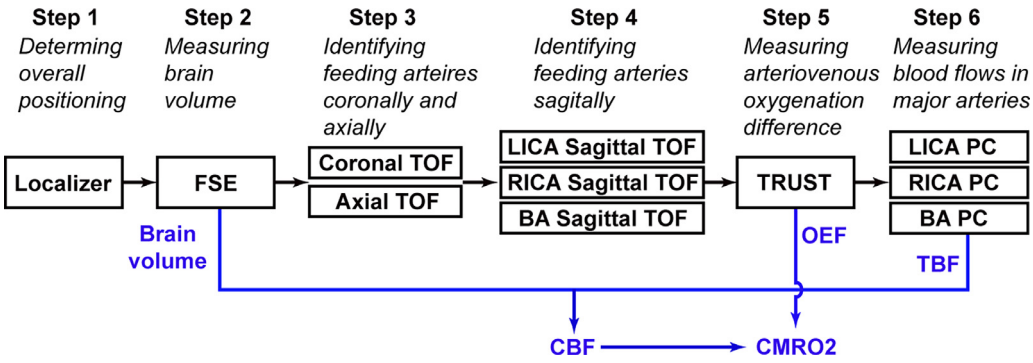

Fig. 1. Schematic diagram of procedures for measuring CMRO2 in mice. The workflow is divided into six major steps. Step 1: localizer scan for visualizing the mouse position within the scanner; Step 2: fast spin echo (FSE) for measuring brain volume; Step 3: time-of-flight (TOF) MRI from the coronal and axial orientations; Step 4: sagittal TOF scans of the three major feeding arteries for brain, namely, left/right internal carotid artery (LICA/RICA) and basilar artery (BA); Step 5: TRUST MRI for measuring OEF; and Step 6: PC MRI of LICA, RICA, and BA for estimating total blood flow (TBF). The unit mass CBF (ml/100g/min) is calculated by normalizing the TBF to brain volume. Finally, CMRO2 is derived using the Fick principle.

Over recent decades, advancements in magnetic resonance imaging (MRI) have enabled non-invasive, non-contrast assessment of metabolic rates in animal brains [4].

T2-relaxation-under-spin-tagging (TRUST) [5] and phase-contrast (PC) [6] MRI offer quantitative evaluations of the oxygen extraction fraction (OEF) and global cerebral blood flow (CBF), respectively. By combining OEF and CBF values, the cerebral metabolic rate of oxygen (CMRO2) can be calculated using the Fick principle [7]. In this study, we describe a step-by-step method for performing TRUST and PC MRI scans in mice at 11.7T scanner, providing a practical framework for non-invasive assessment of global brain metabolism and promisingly offering an alternative for PET when regional pattern is not the primary focus.

Method details

An 11.7 T Bruker Biospec system (Bruker, Ettlingen, Germany) with a horizontal bore and actively shielded pulse field gradient (maximal intensity: 0.74 T/m) was used for imaging. Data were acquired using a 72-mm quadrature volume resonator as the transmitter and a four-element (2 × 2) phased-array coil as the receiver. B0 homogeneity across the mouse brain was optimized using global shimming (up to the second order) based on a subject-specific pre-acquired field map. Mice were anesthetized with 1.5%–2.0% isoflurane for 15 min as an induction. At the 10th min of induction, each mouse was placed on a temperature-controlled, water-heated animal bed and immobilized using a bite bar, ear pins, and a custom-built 3D-printed holder before being positioned within the magnetic. Maintenance isoflurane was typically set at 1.0-1.2% to maintain a respiration rate of 70-120 breaths per minute or adjusted according to the study's purpose.

The procedures for measuring CMRO2 in mice consist of six steps, including reference scans to facilitate slice positioning and measurement scans to quantify parameters related to CMRO2 assessment (Fig. 1).

A fast low-angle shot (FLASH) scan, referred to as the "localizer" on the Bruker Biospec system, is performed first to localize the mouse (Fig. 1). The scan is conducted with the following parameters: repetition time (TR)/echo time (TE) = 120/2.3 ms, field of view (FOV) = 40 × 40 mm^2, matrix size = 256 × 256, slice thickness = 1.0 mm, flip angle = 30°, and scan duration = 0.3 min. Anatomical images are acquired from three orthogonal orientations: axial, sagittal, and coronal (Fig. 2A-C).

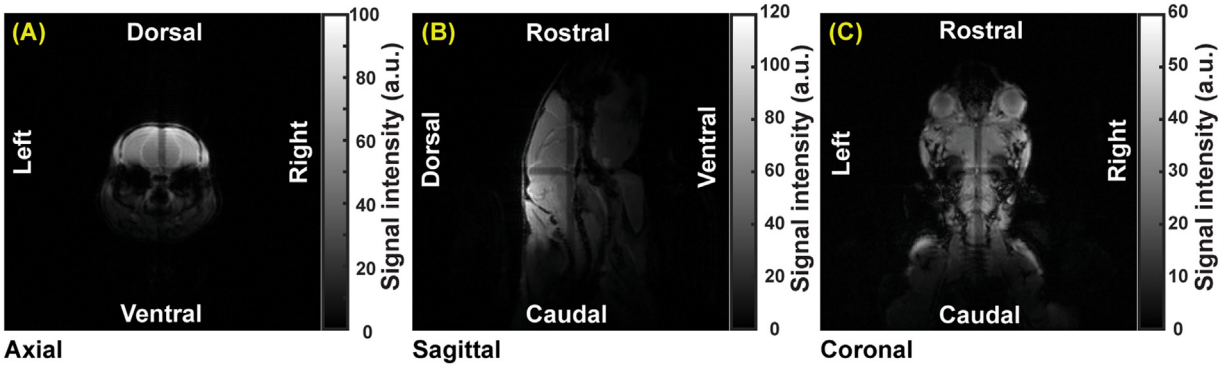

Fig. 2. Localizer images from three orthogonal orientations: axial (A), sagittal (B), and coronal (C) views.

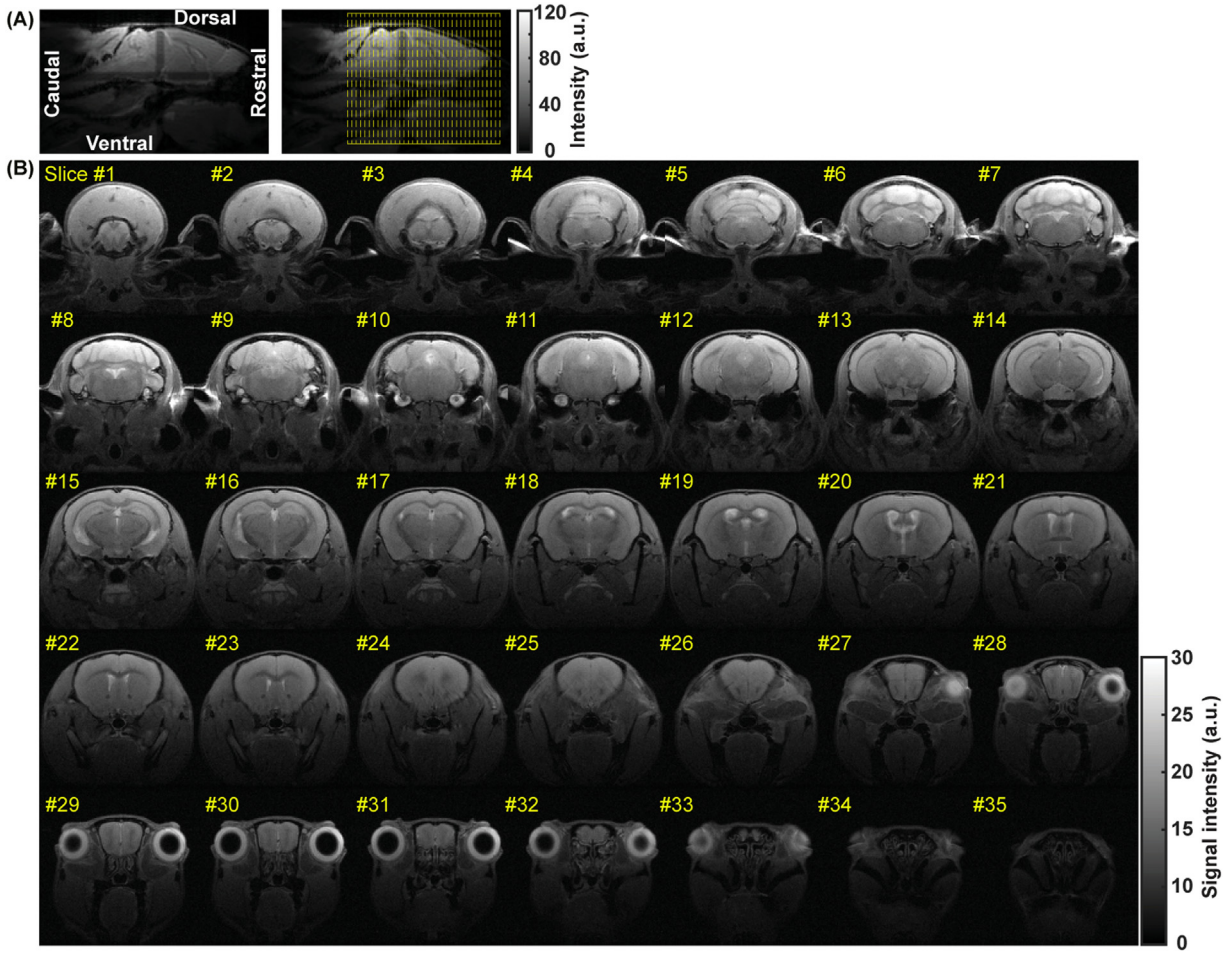

Fig. 3. FSE scan for brain volume measurement. (A) shows the sagittal localizer image (left panel) and the slice geometry of the FSE scan overlaid (right panel). (B) shows FSE images from various axial slices, displayed sequentially from Slice #1 (caudal) to #35 (rostral).

A fast spin echo (FSE) sequence is applied to estimate total brain volume. The scan covers 35 axial slices, as shown in Fig. 3A. The key experimental parameters are as follows: TR/TE = 3000/11.0 ms, FOV = 15 × 15 mm^2, matrix size = 128 × 128, slice thickness = 0.5 mm (no inter-slice gap), echo spacing = 5.5 ms (4 spin echoes per scan), and scan duration = 1.6 min. Fig. 3B displays exemplary FSE images from a mouse. Slice-by-slice manual drawing of regions of interest (ROIs), referencing to the mouse brain atlas (http://atlas.brain-map.org), can be performed to delineate brain regions. The total voxel count within the ROIs determines the total brain volume. ROIs span brain regions from the C1 vertebral spine (caudal side) to the olfactory area (rostral side). Brain weight can then be estimated by scaling brain volume to a tissue density of 1.04 g/ml [8]. Custom-built MATLAB scripts (MathWorks, Natick, MA) for brain volume estimation are available at https://github.com/zyliamwei/MouseCMRO2.

A coronal time-of-flight (TOF) MRI is performed to visualize the major feeding arteries in the coronal orientation. The bottom edge of the brain as shown by the red dotted line in the sagittal localizer image (Fig. 4A) is utilized to guide slice positioning. A total of 9 slices parallel to the bottom edge of the brain are acquired, with one slice positioned just above the brain's bottom edge (Fig. 4A). Key parameters for the coronal TOF scan are: TR/TE = 45/2.6 ms, FOV = 16 [left-right] × 25 [caudal-rostral] mm^2, matrix size = 256 × 256, slice thickness = 0.5 mm, and scan duration = 2.6 min. An exemplary dataset of coronal TOF images is shown in Fig. 4C. Starting from the dorsal side, the basilar artery (BA), characterized by the upside-down "Y" shape, appears first, followed by the left internal carotid artery (LICA) and right internal carotid artery (RICA). The coronal TOF images are used as a reference for subsequent PC scans.

An axial TOF scan is performed after the coronal TOF scan to visualize different components of the sagittal sinuses. The key parameters for the axial TOF are: TR/TE = 20/2.7 ms, FOV = 15 × 15 mm^2, matrix size = 256 × 256, slice thickness = 0.5 mm, 5 slices with no inter-slice gap, and scan duration = 0.3 min. The anatomical "dip" at the dorsal side of the brain, indicated by the red arrow (Fig. 4B), serves as a landmark for slice positioning of the axial TOF. All 5 slices are placed at the rostral side of the dorsal dip (Fig. 4B). The confluence of the sagittal sinuses is identified by comparing the axial TOF images with a vasculature atlas [9]. In Fig. 4D, the confluence of the sagittal sinuses is located in Slice #3, which will be used for the subsequent TRUST scan.

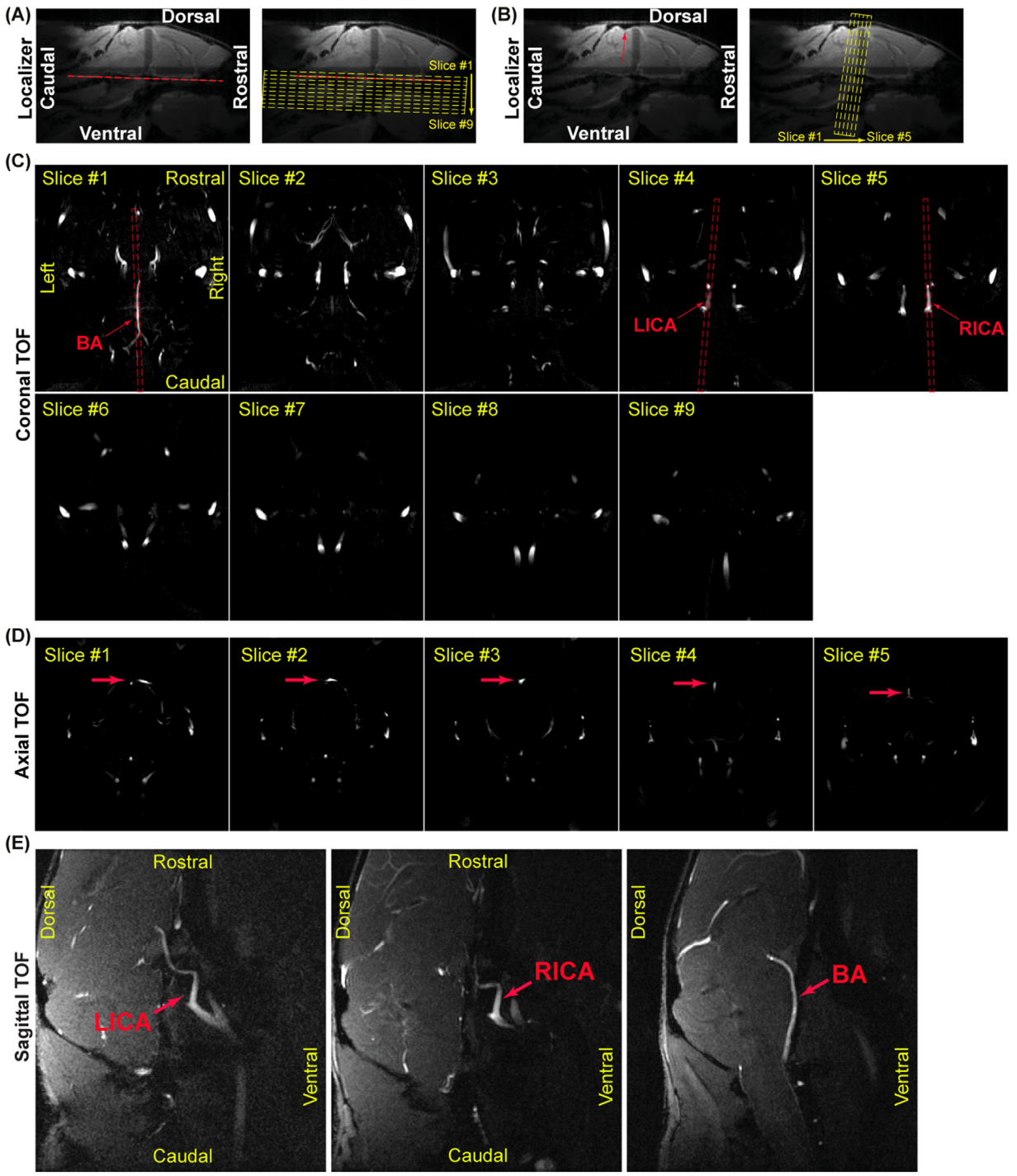

Fig. 4. Implementation of coronal and axial TOF scans. (A) and (B) show the slice geometry of the coronal and axial TOF scans, respectively, overlaid on the sagittal localizer image. (C), (D), and (E) present the coronal, axial, and sagittal TOF images for visualizing vessels, respectively.

Three sagittal TOF scans are performed to provide an additional view of the feeding arteries (LICA, RICA, and BA), enabling the positioning of PC slices to be perpendicular to the vessel trajectories. A single slice is applied to cover the targeted artery based on reference to the coronal TOF images, as indicated by the red dotted box overlaid on Slice #1 (for BA), Slice #4 (for LICA), and Slice #5 (for RICA). Key parameters for the single-slice sagittal TOF are: TR/TE = 60/2.5 ms, FOV = 16 × 16 mm^2, matrix size = 256 × 256, slice thickness = 0.5 mm, and scan duration = 0.4 min. Exemplary sagittal TOF results are displayed in Fig. 4E.

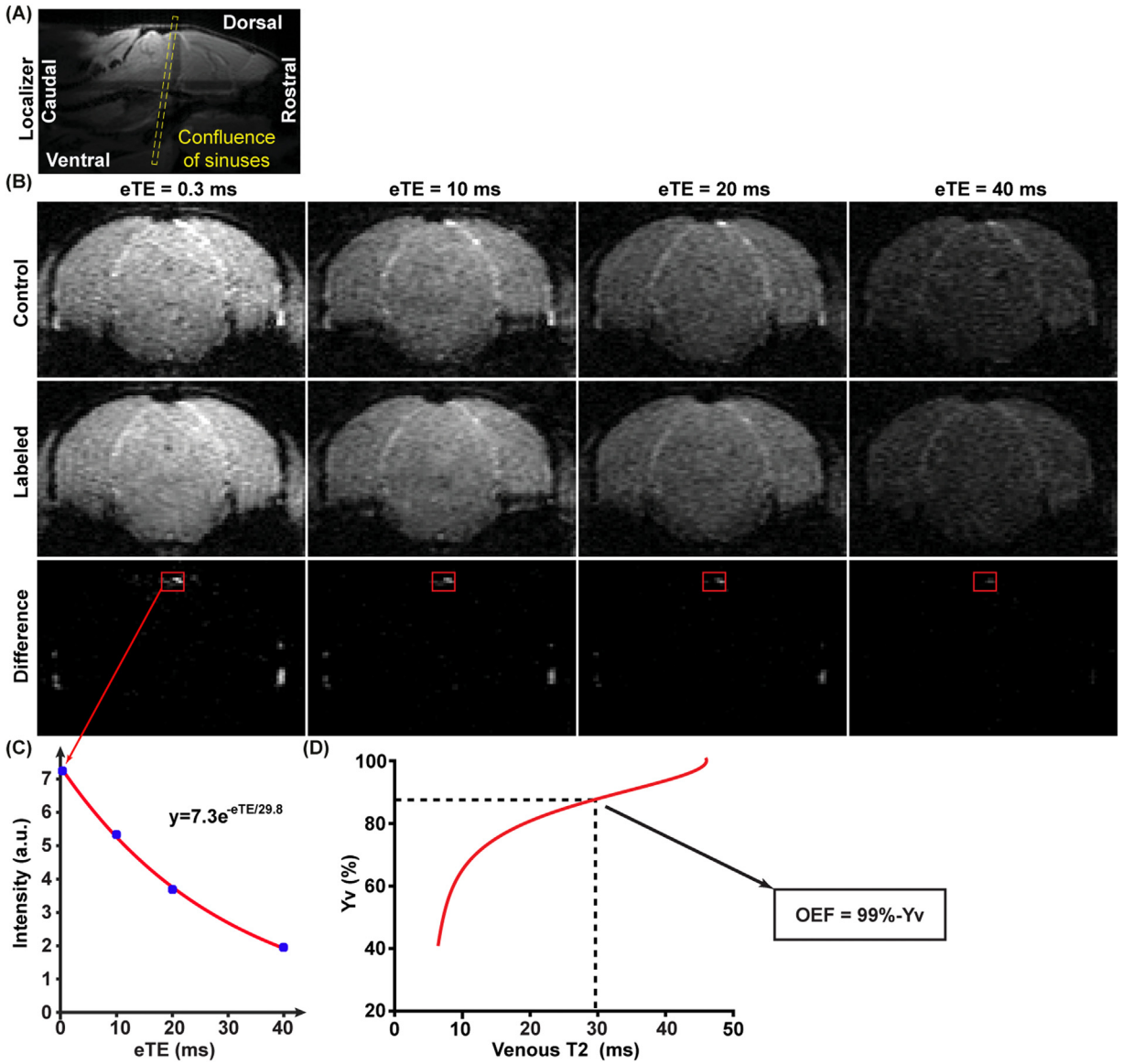

Fig. 5. Implementation of the TRUST MRI. (A) shows the slice geometry of the TRUST scan overlaid on the sagittal localizer image. (B) displays the control, labeled, and difference images at four effective echo times (eTE): 0.3, 10, 20, and 40 ms. (C) shows the monoexponential fitting. (D) illustrates the conversion of venous T2 to venous oxygenation (Yv) and the OEF calculation.

The TRUST scan is performed referencing the axial TOF images, with the imaging slice positioned at the confluence of the sagittal sinuses (Slice #3 in Fig. 4D). Fig. 5A shows the slice geometry of the TRUST scan overlaid on the sagittal localizer image. Key parameters for the scan are: TR/TE = 3500/4.9 ms, FOV = 16 × 16 mm^2, matrix size = 128 × 128, slice thickness = 0.5 mm, inversion slab thickness = 2.5 mm, post-labeling delay = 1000 ms, effective TE (eTE) = 0.3/10/20/40 ms, echo spacing of eTE = 5.0 ms, and scan duration = 5.6 min with a 12-segment gradient-echo echo-planar-imaging (EPI) acquisition. The Pairwise difference between the control and labeled images generates the difference images for each eTE value, as shown in Fig. 5B. To fit the venous T2, an ROI is drawn to encompass the confluence of the sagittal sinuses (marked by red boxes in Fig. 5B), and the four voxels with the highest signal intensities within the ROI are averaged. The signal intensities at different eTE values are fitted to a monoexponential function, i.e., $y = S_0 e^{-\frac{eTE}{T2v}}$, where S_0 represents the theoretical signal intensity at eTE = 0 ms and T2v denotes the transverse relaxation time of venous blood (Fig. 5C). Finally, the measured T2v is converted into venous oxygenation (Yv) [10], allowing calculation of the OEF, which reflects the arteriovenous oxygenation difference. Since arterial oxygenation is typically near 100%, it is assumed to be 99% [11]. The processing of TRUST data can be done using a custom-built graphical user interface (GUI), available at https://github.com/zyliamwei/MouseCMRO2. Note that varying eTE numbers and EPI segments may be used based on specific applications.

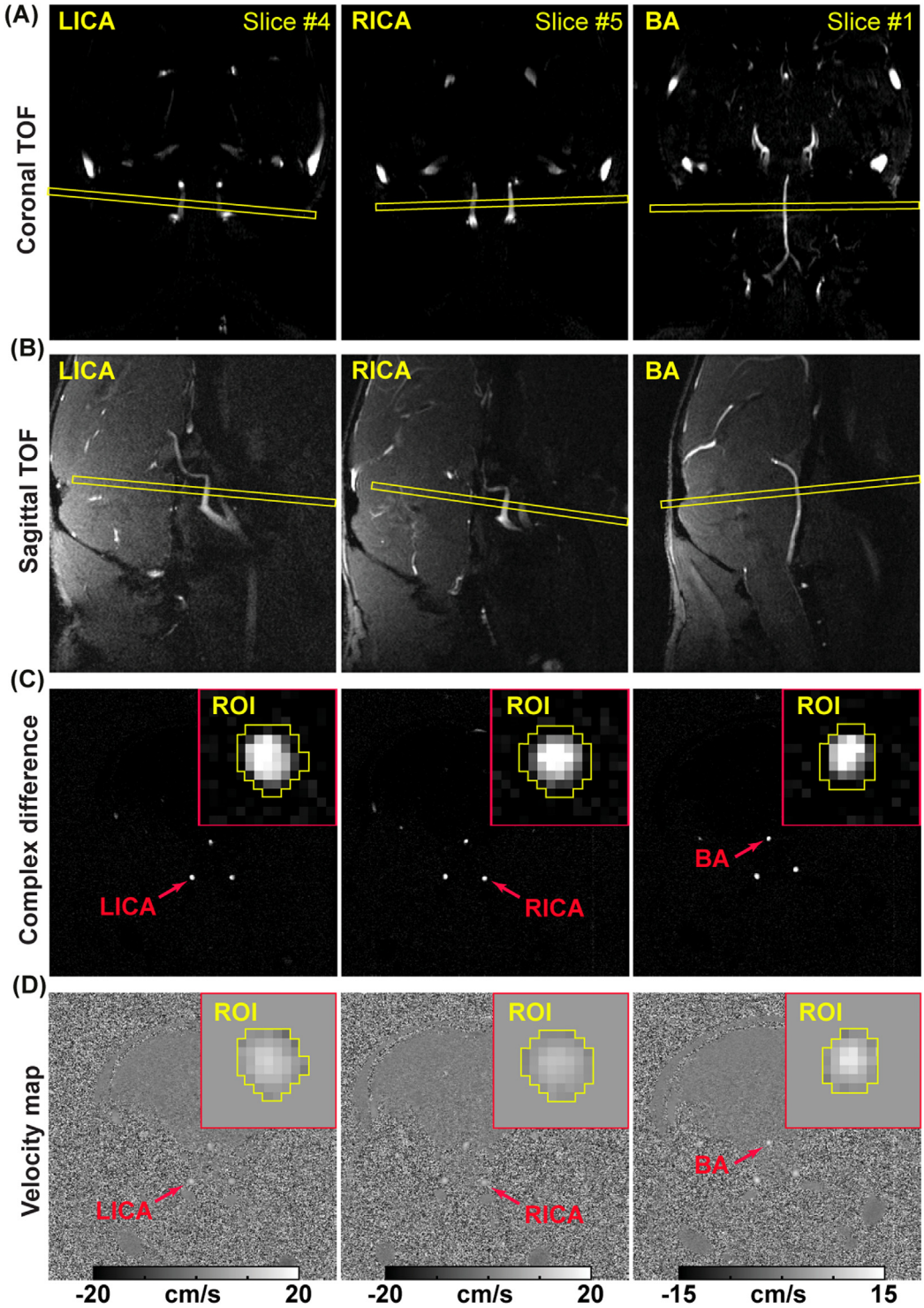

Fig. 6. Implementation of the PC MRI. (A) and (B) show the slice geometry of the PC scan overlaid on the coronal and sagittal TOF images, respectively. (C) displays the complex difference (CD) images of the LICA, RICA, and BA, with the ROI manually drawn on the CD image and zoomed in for clarity (red boxes). (D) shows the velocity maps of LICA, RICA, and BA. The ROIs drawn on CD images are applied to the corresponding velocity maps (red boxes).

In cases where a relatively small T2v is expected, such as during studies of awake CMRO2 (i.e., without inhalational anesthesia), 4 eTE values and 12 EPI segments are used. Alternatively, 3 eTE values and 8 EPI segments can shorten scan duration [12,13].

PC MRI is applied to estimate blood flow with three separate scans targeting the LICA, RICA, and BA, respectively. The imaging slice of each PC scan is positioned perpendicular to the corresponding vascular trajectory using reference to the coronal and sagittal TOF images (yellow boxes in Fig. 6A and B). Key parameters for the PC scan include: TR/TE = 15/3.2 ms, FOV = 15 × 15 mm^2, matrix size = 300 × 300, slice thickness = 0.5 mm, encoding velocity = 20 (for LICA and RICA) / 15 (for BA) cm/s, number of average = 4, dummy scan = 8, receiver bandwidth = 100 kHz, flip angle = 25°, partial Fourier acquisition factor = 0.7, and scan duration = 0.6 min per artery. A ROI is manually drawn on the complex difference (CD) image, where there is excellent contrast between the artery and surrounding tissue (yellow polygons in Fig. 6C). The ROI is then applied to the velocity map, and the integral of blood flow velocities within the arterial region represents blood flow. Summing the blood flows from LICA, RICA, and BA yields the total blood flow (TBF). Finally, CBF is calculated by normalizing the TBF to brain weight and is reported in ml/100g/min. The processing of PC data can be done using a custom-built graphical user interface (GUI), available at https://github.com/zyliamwei/MouseCMRO2.

CMRO2 is calculated according to the Fick principle: $CMRO2 = C_a \cdot OEF \cdot CBF$, where C_a denotes the molar concentration of oxygen in a unit volume of blood. C_a is a constant primarily determined by the haematocrit level or, equivalently, the haemoglobin content, and is assumed to be 882.1 μmol O_2/100ml blood [14]. CMRO2 is expressed in μmol oxygen per 100 g of brain tissue per minute (μmol O2/100 g/min). It is recommended to record respiration rate during the experiments and include respiration rate as a co-variate in statistical analyses [15,16]. On-site processing is recommended to allow the repetition of scans affected by physiological noise, such as cases of unsatisfactory fitting in TRUST data. The parameters of reference scans can be applied to other field strengths (e.g., 9.4T or 7T), provided the image contrast is sufficient to accurately identify structural or vascular landmarks. However, re-optimization of measurement scan parameters may be necessary to account for differences in T1 and T2 relaxation times of MRI signals.

Method validation

The method described here has been extensively validated in the associated technical paper [16] and other related studies [12,17]. The dependence of CMRO2 measurements on neuronal activity levels was investigated in awaking mice, confirming the association between increased high-frequency electroencephalogram (EEG) activity and elevated CMRO2 [16]. Furthermore, the sensitivity of CMRO2 measurement in detecting pathological changes was validated in a mouse model of Alzheimer's disease [17].

Limitations

Our method uses the Fick principle to calculate CMRO2. Since OEF and CBF are measured globally, the method is limited to providing global measurements. Further developments are needed to offer regional information, which would be particularly useful for applications that focus on pattern heterogeneity and regional differences across various brain regions.

Ethics statements

Experiments involved in this study were conducted in accordance with the National Institutes of Health guidelines for the care and use of laboratory animals, as well as the ARRIVE guidelines, and approved by the Johns Hopkins Medical Institution Animal Care and Use Committee. Procedures were carefully designed and conducted to minimize discomfort and stress to the animals.

Declaration of competing interest

The authors declare that they have no known competing financial interests or personal relationships that could have appeared to influence the work reported in this paper.

CRediT authorship contribution statement

Xiuli Yang: Methodology, Software, Validation, Writing – original draft. **Yuguo Li:** Investigation, Writing – review & editing. **Hanzhang Lu:** Conceptualization, Methodology, Resources, Funding acquisition, Writing – review & editing. **Zhiliang Wei:** Conceptualization, Methodology, Software, Resources, Data curation, Funding acquisition, Writing – review & editing.

Data availability

Data will be made available on request.

Acknowledgments

This work was supported by the National Institutes of Health [grant number R01 AG081932 and P41 EB031771].

References

[1] D.F. Rolfe, G.C. Brown, Cellular energy utilization and molecular origin of standard metabolic rate in mammals, Physiol. Rev. 77 (3) (1997) 731–758.
[2] Z. Wei, Q. Wang, H.R. Modi, S.-M. Cho, R.G. Geocadin, N.V. Thakor, et al., Acute-stage MRI cerebral oxygen consumption biomarkers predict 24-hour neurological outcome in a rat cardiac arrest model, NMR Biomed. 33 (11) (2020) e4377.
[3] B.P. Thomas, M. Sheng, B.Y. Tseng, T. Tarumi, K. Martin-Cook, K.B. Womack, et al., Reduced global brain metabolism but maintained vascular function in amnestic mild cognitive impairment, J. Cereb. Blood Flow Metab. 37 (4) (2017) 1508–1516.
[4] D. Jiang, H. Lu, Cerebral oxygen extraction fraction MRI: techniques and applications, Magn. Reson. Med. 88 (2) (2022) 575–600.
[5] H. Lu, Y. Ge, Quantitative evaluation of oxygenation in venous vessels using T2-relaxation-under-spin-tagging MRI, Magn. Reson. Med. 60 (2) (2008) 357–363.
[6] J. Lotz, C. Meier, A. Leppert, M. Galanski, Cardiovascular flow measurement with phase-contrast MR imaging: basic facts and implementation, RadioGraphics 22 (2002) 651–671.
[7] S.S. Kety, C.F. Schmidt, The nitrous oxide method for the quantitative determination of cerebral blood flow in man: theory, procedure and normal values, J. Clin. Invest. 27 (4) (1948) 476–483.
[8] P. Herscovitch, M.E. Raichle, What is the correct value for the brain–blood partition coefficient for water? J. Cereb. Blood Flow Metab. 5 (1) (1985) 65–69.
[9] A. Dorr, J.G. Sled, N. Kabani, Three-dimensional cerebral vasculature of the CBA mouse brain: a magnetic resonance imaging and micro computed tomography study, Neuroimage 35 (4) (2007) 1409–1423.
[10] W. Li, P.C.M. van Zijl, Quantitative theory for the transverse relaxation time of blood water, NMR Biomed. 33 (2020) e4207.
[11] A.L. Lin, Q. Qin, X. Zhao, T.Q. Duong, Blood longitudinal (T1) and transverse (T2) relaxation time constants at 11.7 Tesla, Magn. Reson. Mater. Phys. 25 (3) (2012) 245–249.
[12] Z. Wei, J. Xu, P. Liu, L. Chen, W. Li, P.C.M. van Zijl, et al., Quantitative assessment of cerebral venous blood T2 in mouse at 11.7T: implementation, optimization, and age effect, Magn. Reson. Med. 80 (2) (2018) 521–528.
[13] M. Yao, Z. Wei, J.S. Nielsen, Y. Ouyang, A. Kakazu, H. Wang, et al., Senolytic therapy preserves blood-brain barrier integrity and promotes microglia homeostasis in a tauopathy model, Neurobiol. Dis. 202 (2024) 106711.
[14] J.A. Ulatowski, J.M.E. Oja, J.I. Suarez, R.A. Kauppinen, R.J. Traystman, P.C.M. van Zijl, *In vivo* determination of absolute cerebral blood volume using hemoglobin as a natural contrast agent: an MRI study using altered arterial carbon dioxide tension, J. Cereb. Blood Flow Metab. 19 (1999) 809–817.
[15] Z. Wei, Y. Li, A. Bibic, W. Duan, J. Xu, H. Lu, Toward accurate cerebral blood flow estimation in mice after accounting for anesthesia, Front. Physiol. 14 (2023) 1169622.
[16] Z. Wei, S.E. Roh, X. Yang, W. Wang, J. Wang, L. Chen, et al., The impact of isoflurane anesthesia on brain metabolism in mice: an MRI and electroencephalography (EEG) study, NMR Biomed. 37 (2024) e5260.
[17] Z. Wei, J. Xu, L. Chen, L. Hirschler, E.L. Barbier, T. Li, et al., Brain metabolism in tau and amyloid mouse models of Alzheimer's disease: an MRI study, NMR Biomed. 34 (9) (2021) e4568.